



DLM estimates of long-term Ozone trends from Dobson and Brewer Umkehr profiles

Eliane Maillard Barras¹, Alexander Haefele¹, René Stübi¹, Achille Jouberton², Herbert Schill³, Irina Petropavlovskikh^{4,5}, Koji Miyagawa⁵, Martin Stanek⁶, and Lucien Froidevaux⁷

¹Federal Office of Meteorology and Climatology, MeteoSwiss, Switzerland

²now at Swiss Federal Institute for Forest, Snow and Landscape Research (WSL), Birmensdorf, Switzerland

³Physikalisch-Meteorologisches Observatorium Davos, World Radiation Center, Switzerland

⁴CIRES, University of Colorado, Boulder, CO, USA

⁵NOAA, Global Monitoring Lab, Boulder, CO, USA

⁶Solar and Ozone Observatory, Czech Hydrometeorological Institute, Hradec Kralove, Czech Republic

⁷Jet Propulsion Laboratory, California Institute of Technology, Pasadena, CA, USA

Correspondence: Eliane Maillard Barras (eliane.maillard@meteoswiss.ch)

Abstract.

Six collocated spectrophotometers based in Arosa/Davos, Switzerland, have been measuring ozone profiles continuously since 1956 for the oldest Dobson and since 2005 for the most recent Brewer instrument. The datasets of these 2 ground-based triads (3 Dobsons and 3 Brewers) allow continuous intercomparisons and derivation of long-term trend estimates. In this study, the post-2000 ozone profile trends are estimated from the Dobson and the Brewer Umkehr time series, following a careful homogenization of the Dobson D051 dataset.

Mainly, two periods in the post-2000 Dobson D051 dataset show anomalies when compared to the Brewer triad time series: in 2011-2013, an offset has been attributed to technical interventions during the renewal of the spectrophotometer acquisition system; in 2018, an offset with respect to the Brewer triad and Aura MLS has been detected following a technical intervention on the spectrophotometer wedge. The Dobson D051 time series was homogenized using its difference to the Brewers triad N values time series and the ozone profiles were retrieved from the modified N values by optimal estimation method (OEM). Simultaneously, the Dobson D051 time series was optimized by NOAA relying on the NASA M2GMI model simulations to identify and correct instrumental artifacts in the record. Comparisons of the two homogenized data records show common correction periods and globally similar intensities of the N values corrections.

Long-term trends were estimated by Dynamic Linear Modeling (DLM) from Dobson ozone profile time series and, for the first time, from Brewer ozone profile time series. A positive trend of 0.2 to 0.5 %/year is estimated above 35 km, significant for Dobson D051 but lower and therefore non significantly different from zero at the 95% level of confidence for Brewer B040. As shown on the Dobson D051 data record, the trend seems to become significantly positive only in 2004. Moreover, a persistent negative trend is estimated in the middle and the lower stratosphere with different levels of significance depending on the dataset.



1 Introduction

The stratospheric ozone layer is essential for its role in protecting the Earth's surface from harmful solar ultraviolet radiation. Stratospheric ozone depletion occurring during the second half of the twentieth century has been contained by the strict application of the Montreal Protocol and its amendments (MP1, 1987). While in the upper stratosphere (10–1 hPa, 32–48 km), ozone has started to show significant signs of recovery (e.g. Petropavlovskikh et al., 2019), in the lower stratosphere (147–32 hPa, 13–24 km), measurements show that ozone is still decreasing (Ball et al., 2018). Uncertainties remain for the middle stratospheric trends (32–10 hPa, 24–32 km) with different composites showing different changes giving a picture of a relatively flat trend with low significance (Ball et al., 2018).

Intensive discussions about the significance of the lower stratospheric trends and about the discrepancies between the magnitudes of the model simulated and the measured ozone trends are ongoing in the recent literature. Using TOMCAT 3-D CTM, Chipperfield et al. (2018) pointed to large interannual variability rather than an ongoing downward trend. Wargan et al. (2018) confirms the negative trend in the lower stratosphere (LS) in the northern hemisphere (NH) using DLM on MERRA-2 reanalysis. Sensitivity analyses by Ball et al. (2019) and Dietmüller et al. (2021) support the negative NH LS trends highlighting, for the former, the overestimated magnitude of the final years (-2018) anomalies by the models and, for the latter, the underestimated probability density function of the model trends, as causes for the bad accordance between the simulated and measured ozone LS trends. Orbe et al. (2020) associated the negative NH LS trends with a change in advection, describing a northward upwelling expansion associated with an enhancement of the downwelling over NH mid-latitudes. In this case, the discrepancies in magnitude between the LS trends retrieved from the measurements and from the models (M2GMI and MERRA2 reanalysis) are attributed to an imperfect simulation of the tropical convective processes and of the 2016 inversion of the QBO.

Multilinear regression (MLR) is widely and consistently used for ozone trend estimation. This is the dominant method in the recent and past trend estimate literature (e.g. Petropavlovskikh et al., 2019; Sofieva et al., 2021; Maillard Barras et al., 2020; McPeters et al., 1996a; Reinsel et al., 2002; Tummon et al., 2015; WMO, 1998; Staehelin et al., 2001, and references therein). Trend estimates are obtained by fitting a MLR function to the monthly mean ozone time series, presuming a linear dependence of the ozone content towards the explanatory variables and a linear increase or decrease of the ozone content over time. The sensitivity of the post-2000 trend magnitude towards the time range has been extensively discussed (e.g. Bernet et al., 2019; Dietmüller et al., 2021). Non monotonic post-2000 trends have also been reported in Arosio et al. (2019) where MLR trends are estimated from a merged SCIAMACHY, OMPS and SAGEII dataset on the 2003 to 2018 period. In their study, stratospheric tropical trends are shown to be negative during the 2004 to 2011 period and positive since 2012.

Trend estimates by DLM are recent in the literature. First reports are from Laine et al. (2014) who developed the DLM analysis for trend evaluation and applied it on a merge of SAGEII and GOMOS data records. They compare trend estimates by DLM to trend estimates by piecewise MLR, the latter being described in a companion paper by Kyrölä et al. (2013). They conclude that DLM is a robust method well suited for modeling ozone time series changes (see Section 4.2). Their results show a statistically significant turnaround in the ozone time series after 1997 at mid-latitudes in the 35 to 55 km altitude range and a more complex behavior of the ozone concentration than the description which can be made by a simple piecewise multilinear



55 regression model. Consequently, stronger ozone variations (decrease or increase) are reported locally when estimated by DLM
than by MLR. Ball et al. (2017) applied DLM on a Bayesian composite (BASIC) of satellites data records. The changes in
ozone between 1998 and 2012 estimated using DLM indicate a clear and significant ozone recovery in the upper stratosphere
(UpS). DLM has also been used to estimate trends in the LS based on the merged SWOOSH/GOZCARDS data records (Ball
et al., 2018) as discussed previously. More recently, DLM trend estimates on SOS (SageII, Osiris and SAGEIII) merged satellite
60 data record have been reported (Bognar et al., 2022) and indicate a clear UpS ozone recovery with varying turnaround years
depending on the latitude, a decrease since 2012 in the NH upper/middle stratosphere, but without excluding a step in the Osiris
dataset as a cause, and a persistent decrease in the tropical LS.

Dobson Umkehr ozone profile data record have been extensively used in the pre-1998 stratospheric trend estimates (Reinsel
et al., 1989; Randel et al., 1999; Miller et al., 1995). Beginning in 1956 for the oldest, the Umkehr records were unique at
65 that time since satellites records only became available in 1979 (McPeters et al., 1996b; Bhartia et al., 2013) and radiosondes,
starting in 1960 (Smit et al., 2007), do not reach the UpS. Few studies based exclusively on Umkehr measurements report on
post-2000 stratospheric ozone trends (Zanis et al., 2006; Park et al., 2013). Zanis et al. (2006) derived trends from the Arosa
Dobson Umkehr dataset and reported statistically significant negative trends in the 1970 to 1995 period, and the first signs of a
reversing trend in the lower and the upper stratosphere for the period 1996 to 2004. Since this turnaround was not statistically
70 significant, the authors suggested that the dataset should be reevaluated at a future stage when more measurements become
available. The Dobson Umkehr dataset was then corrected in 2008 for technical issues (Maillard et al., 2008) and ozone profiles
were reprocessed from corrected observations (N values). The homogenized Umkehr time-series was used by Park et al. (2013)
to derive trends using functional mixed models, and in the frame of the LOTUS project (Petropavlovskikh et al., 2019), which
derived stratospheric ozone trends from improved and combined datasets (satellites, ground-based and models). The trends
75 derived from the Umkehr datasets are in accordance with trends derived from other ground-based instruments for the pre-1997
period and the post-2000 period. Umkehr data corroborate also the satellite findings showing highly statistically significant
evidence of declining ozone concentrations since the mid 1980s in the UpS and post-2000 positive trends ranging between
2.0% and 3.1% per decade in the UpS of NH mid-latitudes. The Umkehr data records are still extensively used for trend
estimates along with datasets from other ground based techniques, satellites and models (Steinbrecht et al., 2017; Harris et al.,
80 2015; Petropavlovskikh et al., 2019; Tarasick et al., 2019). However, to the authors' knowledge, no trend estimate including
explanatory variables and based on the Brewer Umkehr data records has been reported in the literature so far. A study using
simple linear regression applied to data from the Brewer 005 of Thessaloniki presented by Fragkos et al. (2018) reports 1997-
2017 statistically significant positive trends above 35 km of 0.3%/year and non statistically significant trends below.

The dataset quality is of primary importance for trend studies, and multi-instrument comparison analyses is suited to assess
85 the long-term stability of data records by estimating the drift and bias of instruments. A reprocessing and a homogenization of
Dobson total ozone (TCO) data record is in progress with consideration of the effects of the relocation from Arosa to Davos
(Stübi et al., 2021b) and the use of ozone absorption cross section from Serdyuchenko et al. (2014) (Gröbner et al., 2021). The
complete homogenization of the Dobson (D051) Umkehr data record is described in this paper.



The paper is organized as follows: the data sources used in this study are described in section 2, with a special focus on the Umkehr method description. In section 3, the complete homogenization of the Dobson D051 Umkehr data record is detailed and compared to the homogenization performed by NOAA in the frame of the ESA project WP-2190 (Garane et al., 2022). The trend estimate methods are described in section 4. DLM trend estimate results are presented and discussed in section 5, followed by conclusions in section 6.

2 Data Sources

2.1 Umkehr data records from Arosa/Davos

TCO and ozone profile measurements with Dobson (and Brewer) spectrophotometers were performed at Arosa from 1926 (and 1988) to 2021 and at Davos since 2012. For a detailed description of the Dobson and Brewer spectrophotometers, we refer to Stübi et al. (2021a, 2017a). The progressive relocalisation of the Dobson and Brewer triads from Arosa to Davos (13 km north of Arosa and 260m lower in altitude) between 2012 and 2021 is described and analyzed in Stübi et al. (2017b, 2021b). Umkehr measurements (see Section 2.2) are performed under clear sky and low cloud cover conditions twice a day since 1956 by Dobson spectrophotometers (Dobson D015 since 1956 and then Dobson D051 since 1988), 4–6 times per month by Dobson 101 since 1988 and by Dobson 062 since 1998. Dobson D051 performs fully automated Umkehr measurements since 1988. The Dobson Umkehr measurements are complemented by Brewer Umkehr measurements since 1988 with Brewer B040 and since 2005 with Brewers 072 and 156. Ozone profile Umkehr measurements initiated in 1956 at Arosa and continued since 2021 at Davos, Switzerland, form the longest continuous Umkehr measurement time series world-wide (Staehelin et al., 2018).

At Arosa, the Dobson D051 sat on a turntable in a conditioned hut maintained at 25-28°C. An aperture in the roof, which opened and closed according to solar zenith angle (SZA) and weather conditions, allowed zenith measurements. The continuous and automated measurements (2 min cycle) are interpolated to 12 nominal solar zenith angles (SZA) and profiles are retrieved using OEM from ground to 50 km. Manual Umkehr measurement started in 1968 with the Dobson D101 and in 1992 with the Dobson D062 as redundant measurements to check the stability of Dobson D051. These are made two to three times each month since 1988 and 1998 in favourable weather conditions. The Dobson D062 and the Dobson 101 have been automated in 2012 and in 2013, respectively (Stübi et al., 2021b). They are located since 2021 in Davos in a common air conditioned container side by side with the Dobson D051, and measure Umkehr curves through a quartz dome. While the Dobson D051 was dedicated exclusively to Umkehr measurement until February 2013, the present set-up allows both direct sun and zenith Umkehr measurements with the three Dobsons. The Arosa/Davos Dobson instruments are regularly calibrated against the two European regional secondary reference Dobson instruments D064 from the Hohenpeissenberg Observatory (MOHp, Germany) and D074 from the Solar and Ozone Observatory in Hradec Králové (SOO-HK, Czech Republic) (Stübi et al., 2021b, Fig. 3).

The Brewer triad consists of two Brewer Mark II single-monochromator instruments, the Brewer B040 and the Brewer B072, and one Brewer Mark III double-monochromator instrument, the Brewer B156. The three instruments measure daily in Umkehr mode when the sun is at the 12 nominal SZAs. Since the operation of the first Brewer at Arosa in 1988, biennial calibrations have been carried out (Stübi et al., 2017a, Fig. 1) towards the traveling reference instrument Brewer 017 and,



since 2008 towards the traveling reference instrument Brewer 185. The instruments of the Brewer triad underwent very few technical interventions and are in good agreement with the travelling references (TCO deviations $\leq 1\%$, (Stübi et al., 2017a)). In particular, no technical issues are reported around 2011-2013 and 2018, which are data records periods considered in the frame of the Dobson D051 homogenization. However, sporadic instabilities in the Brewer B072 data record have been observed while no particular technical issues have been detected by the intercomparison procedures. The Dobson D051, the Brewer B072 and the Brewer B156 have been simultaneously relocated from Arosa to Davos in September 2018 however with an effect on the TCO level within the instrumental noise (Stübi et al., 2017a, 2021b).

2.2 The Umkehr method

The Umkehr method is based on the measurement of the ratio of the zenith-sky UV intensities at two wavelengths in the UVB-UVA range from 300 nm to 330 nm (Huggins absorption band) subject to different strengths of ozone absorption. This ratio is changing as a function of SZA during sunset and sunrise. As the SZA is decreasing from 90° to 60° , the two intensities decrease, the shorter wavelength intensity decreasing more rapidly than the longer wavelength intensity. When the effective scattering height for the shorter wavelength is above the ozone layer, its intensity decreases less rapidly because of the absorption occurring mostly after the scattering event. The ratio shows therefore a maximum at high SZA called the Umkehr effect (Mateer, 1965).

2.2.1 Measurements by Dobson spectrophotometer

The logarithm of the ratio of the two wavelengths (R values) is converted to radiance using calibration tables and reported as N values (Fig.1a) in N-units for 12 nominal SZAs between 60° and 90° (60° , 65° , 70° , 74° , 77° , 80° , 83° , 85° , 86.5° , 88° , 89° and 90°). The nominal wavelength pairs used in a Dobson spectrophotometer are A: 305.5 & 325.4 nm, C: 311.45 & 332.4 nm, and D: 317.6 & 339.8 nm. Two narrow slits separate the respective wavelengths. The ozone profiles (Fig.1b) are retrieved from the measurements of the C pair intensity while the total column measurement requires a combination of 2 wavelength pairs (AD) (Stübi et al., 2021a).

The 12 N values (further called N curve) are screened for clear sky conditions and corrected for cloud influence using a nearby UV/VIS lux meter. This empirical correction is based on the relation between the UV/VIS intensity of clear days (within the same month, for each SZA) and the UV/VIS intensity variation during the cloudy N curve measurement (see Basher, 1982). This cloud correction is based on a uniform cloud layer and may fail for more complicated cloud structures. Haze correction is not included. For these reasons, only profiles retrieved from N curves without any cloud correction or with a small correction are considered for our study.

2.2.2 Measurements by Brewer spectrophotometer

The intensity of 8 wavelengths (306.3, 310.1, 313.5, 316.8, 320.1, 323.2, 326.5, and 329.5 nm) are quasi-simultaneously measured for solar zenith angle changing from 60° and 90° . A holographic grating is used as dispersive element for the solar radiation passing then through narrow slits centered on the desired wavelengths. Mk II Brewer instruments use one single

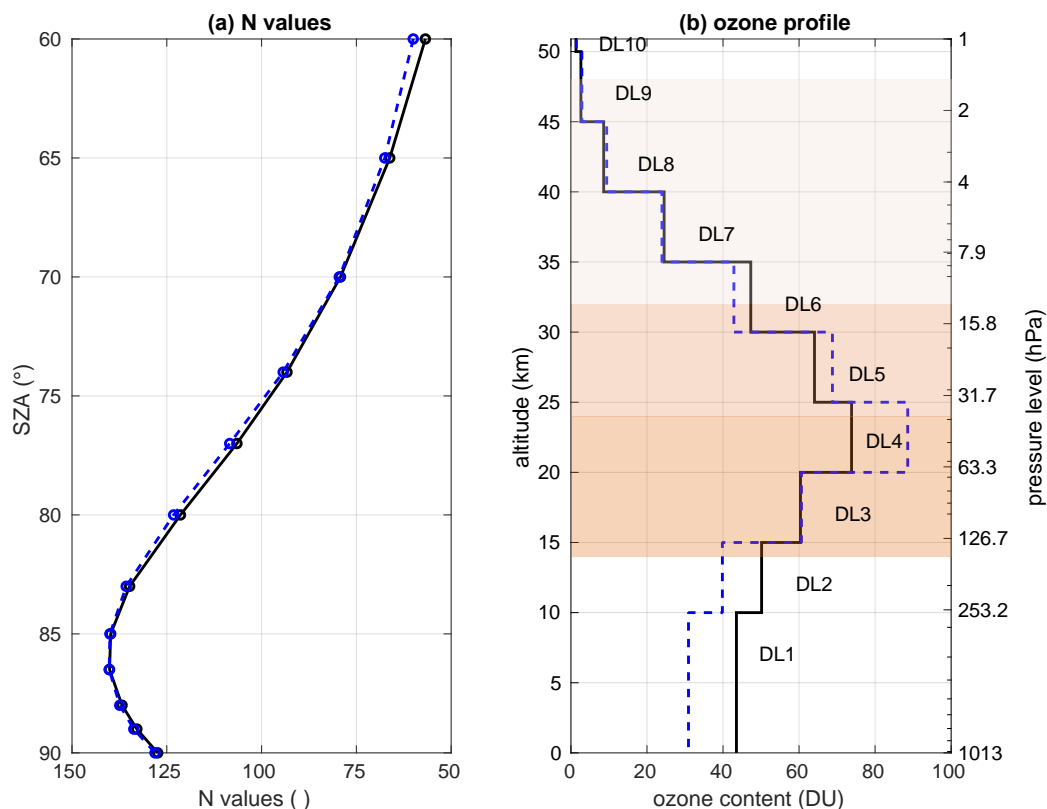


Figure 1. Two examples of N curves at 12 nominal SZAs and their corresponding retrieved ozone profiles in DU in function of altitude in km and pressure level in hPa. Altitude ranges of the 10 Dobson layers (DL) are indicated. Lower, middle and upper stratospheric ranges are displayed in shades of orange.

holographic grating and therefore only one dispersive element to separate the wavelenths. Mk III Brewer instruments are double monochromators that use two holographic gratings (Staehelin et al., 2003). The Umkehr ozone profile is commonly
155 retrieved directly from the absolute wavelength intensities (photocounts at the selected wavelength) by OEM. For similarity with the Dobson Umkehr measurement, the intensity ratio of only two wavelengths are used : 310.05 nm of short set of wavelengths, and 326.5 nm of the long set of wavelengths. The data are flagged for clouds before the interpolation onto the 12 nominal SZA. The quality filter eliminates data points that fall outside a predefined error envelope determined by the range of natural variability and a mean offset.

160 Dobson and Brewer ozone profiles are retrieved by OEM (Rodgers, 2000). The Dobson Umkehr retrieval algorithm is described in Petropavlovskikh et al. (2005a) and the Brewer Umkehr retrieval algorithm has been adapted by Petropavlovskikh et al. (2005b) from the Dobson algorithm. The version of the code used in this study has been implemented by M. Stanek and



can be found at <http://www.o3soft.eu/o3bumkehr.html>. Ozone profiles are given on ten layers between 0 and 50 km with a vertical resolution of 10-15 km. Dobson and Brewer Umkehr retrievals are using the same a priori profile, the ML climatology, described in McPeters and Labow (2012) formed by combining data from Aura MLS (2004-2010) with data from balloon radiosondes (1988-2010). The measurement error covariance matrices are diagonal with values between 0.16 to 0.8 N-units for Dobson and 0.6 to 2 N-units for Brewer. The Brewer observation errors have been estimated by the standard deviation of the 2005–2018 climatological difference of collocated and simultaneous N values measurements. The Averaging Kernels (AVKs, not shown) show that for both instruments, the information below Dobson Layer (DL) 4, peaking at 20 km, is not independent. A generic stray light correction can be applied to reduce systematic biases in the Dobson Umkehr retrieved profiles (Petropavlovskikh et al., 2011).

The Dobson D051 Umkehr observations dataset is regularly archived at the World Ozone and Ultraviolet Radiation Data Centre (WOUDC, www.woudc.org). The Brewers are part of the eubrewnet (<http://www.eubrewnet.org/eubrewnet>), where raw data files are available for registered users.

2.3 NOAA Dobson Umkehr data records (Boulder and OHP)

The Umkehr data record from Boulder is automated using the NOAA WinDobson operational software (Evans et al., 2017) that schedules zenith sky observations at C-pair spectral channels during the morning and afternoon hours. The software uses the near-IR cloud detector to screen the Umkehr data for clear sky conditions. Screened observations are interpolated to 12 nominal SZAs and total column ozone information is added. Data processing includes checks of the retrieved ozone profiles for quality flags and against station climatological variability (± 2 standard deviations). NOAA Dobson Umkehr operational ozone profile data are posted on the GML archive <https://gml.noaa.gov/aftp/data/ozwv/Dobson/AC4/Umkehr/>. The Umkehr observations are archived at WOUDC where the centralized data processing is done by the python-based version of the UMK04 processing software (<https://github.com/woudc/woudc-umkehr>). (Petropavlovskikh et al., 2022).

2.4 Aura MLS

The Microwave Limb Sounder (MLS) is a microwave limb-sounding radiometer on board the Aura Earth observing satellite, launched in July 2004. Ozone profiles are retrieved from Aura MLS radiance measurements at 240 GHz. Details about the instrument can be found in (Waters et al., 2006). In this study we use ozone profiles from the version 4.2 dataset given on 55 pressure levels from 1000 to $1\text{e-}5$ hPa (Livesey et al., 2018). However, the useful vertical range for Aura MLS ozone leads us to only consider Aura MLS data from 10 to 75 km (in this range, the Aura MLS vertical resolution is about 2.5 to 4 km) for Aura MLS overpasses above Switzerland (46.82° N, 6.95° E, $\pm 3^\circ$ in latitude and $\pm 5^\circ$ in longitude). These ozone profiles are interpolated on the Umkehr pressure levels p_i and converted to DU following Ziemke et al. (2017):

$$X_{DU} = C * \bar{X} * (p_i - p_{i-1}) \quad (1)$$

with $C = 0.00079\text{DUhPa}^{-1}\text{ppbv}^{-1}$ and \bar{X} the ozone mean VMR in ppbv. Approximative height is given following the Umkehr layers definition (Petropavlovskikh et al., 2022).



195 3 Homogenization of Dobson D051

While the 2008 homogenization dealt with the Dobson D015 to Dobson D051 transition (using one year of parallel measurements) and with correction of shaft encoder mispositioning on the raw data level, this study deals with a complete homogenization of the Umkehr Dobson D051 time series by comparison to the datasets of the 5 collocated instruments (2 Dobson and 3 Brewer spectrophotometers) on the N value level. The purpose is to detect common anomalies in the difference between
200 Dobson D051 and each of the redundant measurements and to correct the Dobson D051 time series accordingly. However, a correction is only applied if it correlates with a technical issue in the metadata. If we cannot see any indication in the meta data for an instrumental drift, no correction is applied.

Figure 2 shows the time series of monthly mean ozone profile differences between Dobson D051 and the 5 collocated spectrophotometers. Only simultaneous measurements, flagged for bad weather conditions, volcanic eruptions, and for retrieval
205 iterations higher than 3, are considered. The relative differences of the anomalies in % lie within $\pm 15\%$. The comparisons with the Brewer instruments show a seasonal cycle with differences slightly bigger in summer than in winter (not shown; DL6: -2% in winter and $+2\%$ in summer). A similar behavior has been found by Gröbner et al. (2021) when comparing TCO from Dobsons to Brewers. Note that the annual cycle is not visible on the representation of deseasonalised anomalies as in Figure 2.

210 If we focus on the post-2000 period, where we have a precise chronology of the technical interventions, several systematic anomalies can be attributed to technical issues of the Dobson D051 (periods in black frames in Figure 2):

- before 2003 for the altitude range below 30km: the Dobson D051 ozone values are higher than the values measured by the collocated instruments below 20km and lower between 20 and 30 km
- in winter 2010 above 40 km, the Dobson D051 ozone values are higher than the values measured by the collocated
215 instruments
- between 2011 and 2013 in most part of the altitude range, the Dobson D051 ozone values are lower than the values measured by the collocated instruments
- after 2018, the Dobson D051 ozone values are higher than the values measured by the 3 collocated Brewer instruments.

220 The comparison of Dobson D051 with the collocated Dobsons around 2014 and after 2018 are to be taken with caution due to the very limited number of measurements of Dobson D051 in 2014 and of Dobson D062 and Dobson D101 during these periods.

Table 1 summarizes the Dobson D051 problematic periods, the technical issue reported at these periods, and the time ranges and redundant datasets used for the offsets determination.

225 When systematic for each pair of instruments and if related to an instrumental issue, the detected Dobson D051 problematic periods are shifted according to the mean difference with the 3 Brewers or the 2 Dobsons datasets before and after the problematic periods (periods of 2 years are considered). The homogenization is performed on the raw data level (N values) and the ozone profiles are then retrieved from the corrected N values.

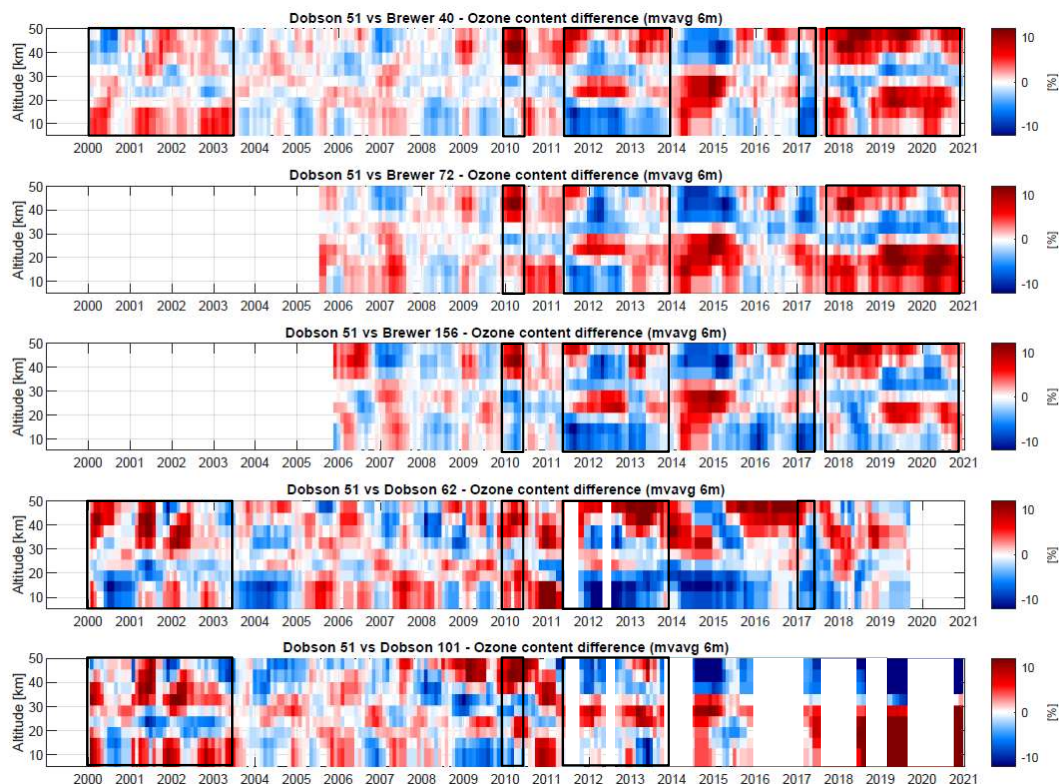


Figure 2. Monthly mean time series of the ozone profiles relative differences for each of the 5 spectrophotometers with respect to D051. The time series are deseasonalized and smoothed by a 6 months moving average.

For each period that requires a correction (black frames in Fig. 2) we apply to the N values a SZA dependent offset which is constant over the period to be corrected. The offset is calculated such that the difference averaged over the period and over the reference instruments (2 Dobsons in 2003 or 3 Brewers after 2011) matches the difference averaged over 2 years before and 2 years after the period and over all reference instruments (see Fig. 3):

$$\Delta_{SZA} = \text{mean}(\Delta_{1SZA}, \Delta_{3SZA}) - \Delta_{2SZA} \quad (2)$$

$$N_{SZA}^{corr} = N_{2SZA} - \Delta_{SZA} \quad (3)$$



Dobson D051 problematic period	Technical issue	Time range of homogenization	Time range used for the offset determination	Redundant datasets used for the offset determination	Comment
1988	D15 to D51	Before 1988.01.01	1987.01.01 - 1988.01.01 and 1988.01.01 - 1989.01.01	D015 and D051 simultaneous measurements	
2003	Intercomparison and new RtoN table New RtoN table considered	Before 2003.07.19	2001.07.19 - 2003.07.19 and 2003.07.19 - 2005.07.19	D062 and D101 mean values	
2010	-	2010.01.01 - 2010.06.30	-	-	Does not correspond to any technical issue. Period limited to 6 month. Not corrected.
2011-2013	New electronics (2011.03.21) New Qlever motors (2012.02.15) New software 3V3 (2013.03.26)	2011.04.01 - 2013.04.01	2009.04.01 - 2011.04.01 and 2015.04.01 - 2017.04.01	B040, B072 and B256 mean values	2014 not considered (number of measurement low and problematic period). Refurbishment of the electronics (HV, motors, feedback loop, amplification board) and position of Q2-lever in function of the room Temperature.
2018	New wedge steel band (2018.05.06) IC(2018.08.07-17): adjustments on optics AROSA to DAVOS (2018.09.28)	Before 2018.05.01	2016.05.01 - 2018.05.01 and 2018.05.01 - 2020.05.01	B040, B072 and B256 mean values	The optical attenuator consists of a moving neutral-density filter (the optical "wedge") attached to a graduated rotating disc (R dial). The wavelength pair selection is achieved by rotating a pair of quartz plates (Q1 lever, Q2 lever) through which the light beam passes.

Table 1. Dobson D051 homogenization description: problematic periods, technical issues, time ranges for homogenization and for offset calculation, used redundant datasets, details of technical issues

235 Δ_{SZA} is the offset between the 3 Brewers mean N values and the Dobson D051 N values for each SZA, Δ_{1SZA} and Δ_{3SZA} are the difference between the 3 Brewers mean N values and the Dobson D051 N values before (period P_1) and after (period P_3) the Dobson D051 problematic period (period P_2). All values are averaged over 2 years periods. N_{SZA}^{corr} is the corrected N value in period P_2 .

In case of a step in the time series (e.g. in July 2003 and in May 2018), the period P_2 does not exist and should not be
 240 considered in Fig. 3. The corrected N value N_{SZA}^{corr} of period P_1 is then obtained following equations 4 and 5.

$$\Delta_{SZA} = \Delta_{1SZA} - \Delta_{3SZA} \quad (4)$$

$$N_{SZA}^{corr} = N_{1SZA} - \Delta_{SZA} \quad (5)$$

In parallel, a homogenization and a correction for the stray light effect of the same Dobson dataset has been performed
 245 by NOAA, using comparison with the M2GMI model on the N values level. A summary of the homogenization method is presented here, for details on the method and for the description of the stray light correction, we refer to Petropavlovskikh et al. (2022).

The NASA Global Modeling Initiative chemistry transport model (GMI CTM) is an off-line model driven by MERRA2 meteorological reanalysis (Gelaro et al., 2017). M2GMI output is driven by a specified dynamics simulation instead of using
 250 MERRA-2 meteorology (Orbe et al., 2017). The ozone and temperature profiles are simulated by the M2GMI model for the Arosa station location. The simulated temperature profile is used for accounting the temperature dependence of the ozone

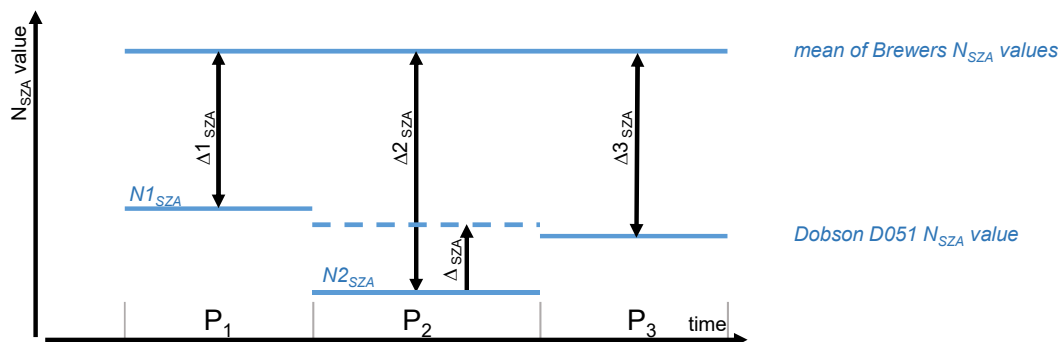


Figure 3. Schematic of the Dobson D051 MeteoSwiss (MCH) homogenization principle

cross section and allows the model to better fit to the day-to-day variability of the N values. The Umkehr retrieval forward model is forced to match this reference and outputs Umkehr N values simulated for an idealized Dobson instrument. For each SZA, differences between simulated and measured Umkehr N-values are averaged over the time between two consecutive
255 calibrations (performed at each intercomparison) of the Dobson D051 to create an empirical correction for the Umkehr curve simulated by the forward model. This correction is then applied to the N values curves which are retrieved by OEM to get optimized ozone profiles. An iterative modification of the N value correction is performed in order to minimize the mean bias to Aura MLS in the 2005–2018 period. While the first iteration of the homogenization remove artificial steps in the Umkehr ozone profile records, the iterative part reduces the bias relative to other ozone observing systems.

260 The NOAA homogenization has been developed to remove artificial steps in the NOAA Umkehr ozone profile records and to reduce the bias relative to other ozone observing systems. Our approach is different in that the homogenization process aims to remove artificial steps in the Dobson D051 Umkehr profiles record by ensuring the independence (in absolute values) of the datasets towards the collocated instruments datasets.

Figure 4 shows the time series of the N values correction as a function of SZA as determined by the NOAA homogenization
265 (Fig. 4a) and by the MCH homogenization (Fig. 4b, this study). For comparison purpose, the NOAA correction values have been offsetted with their mean difference after 2018.

The main differences between the two homogenizations are the variability of the corrections values and the correction of the volcanic eruptions periods. The high variability of the NOAA N values correction comes from the contribution of the stray light effect correction to the total N values correction. This is not corrected for in our N value homogenization. The years around
270 1982 and 1992 are periods of volcanic eruptions (El Chichon and Pinatubo) which are corrected by the NOAA homogenization but flagged in the MCH homogenization as the Umkehr retrieval does not account for the change in atmospheric scattering due to aerosols injection (Petropavlovskikh et al., 2022). For the 1988 to 2003 period, both homogenizations differs for the 77–83°

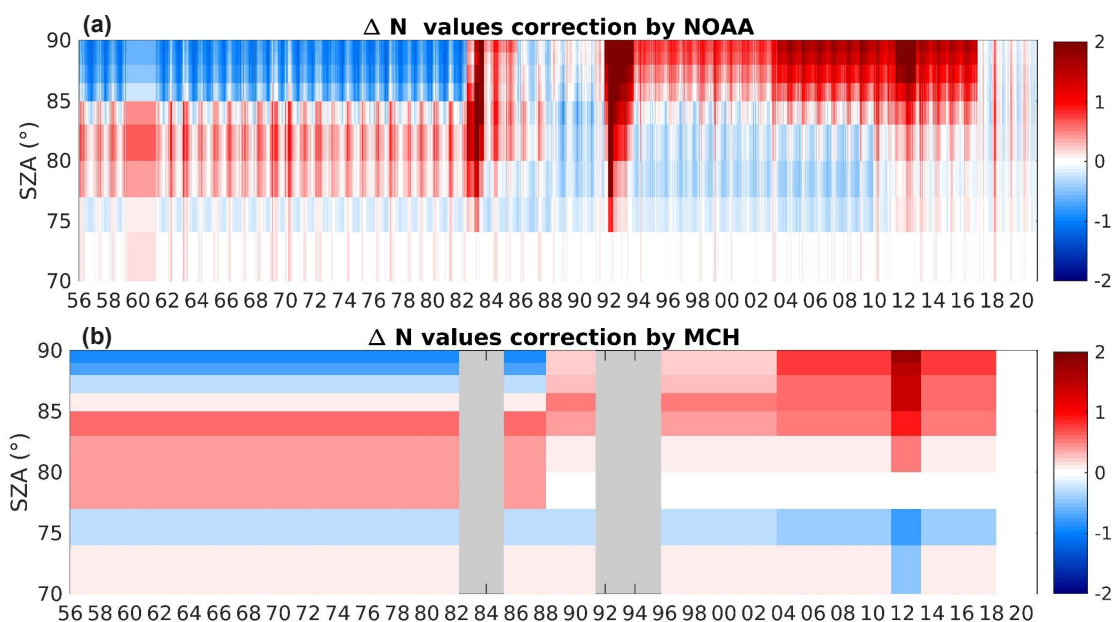


Figure 4. Monthly mean time series of the N values correction (a) for the NOAA and (b) for the MCH homogenization of Dobson D051 dataset. Volcanic eruptions periods (grey shaded area) are not corrected by the MCH homogenization.

SZAs. Otherwise, the correction amplitudes are similar, and their occurrences coincide within a few months in January 1988, in July 2003, in April 2011 to 2013, and in 2010; this is remarkable given the differences in the detection method. Note that
275 the 2010 six-months step has been chosen to be left uncorrected in the MCH homogenization due to the absence of confirmed technical issue at that time. In 2017/2018, the start date considered for the NOAA homogenization is January 2017, while the start date considered by the MCH homogenization is May 2018 with the probable effects of the wedge steel band replacement on the measurements.

However, while both corrections of the N values looks similar, small differences in the N curve shapes can lead to larger
280 differences in the ozone profiles due to the non linear relationship between the N values and the ozone values (see Fig.1 for an example).

In order to evaluate the effects of both homogenization on the Dobson D051 time series, monthly mean relative difference to Aura MLS data record are plotted in Figure 5 for 2 altitude levels i.e. DL5 (25 km) in MS and DL8 (40 km) in UpS. The relative difference of the Brewer B040 time series is also shown for the same layers.

285 The Brewer B040 relative difference shows a constant offset to Aura MLS but clear anomalies in 2012 and 2013 in DL5. The Dobson D051 optimized by NOAA shows a very good accordance with Aura MLS both in DL5 and DL8. The small overall offset value is a result of the optimization procedure which includes an iterative accordance of the 2005–2018 mean towards Aura MLS. No clear offset in the difference to Aura MLS between the NOAA and the MCH homogenized record

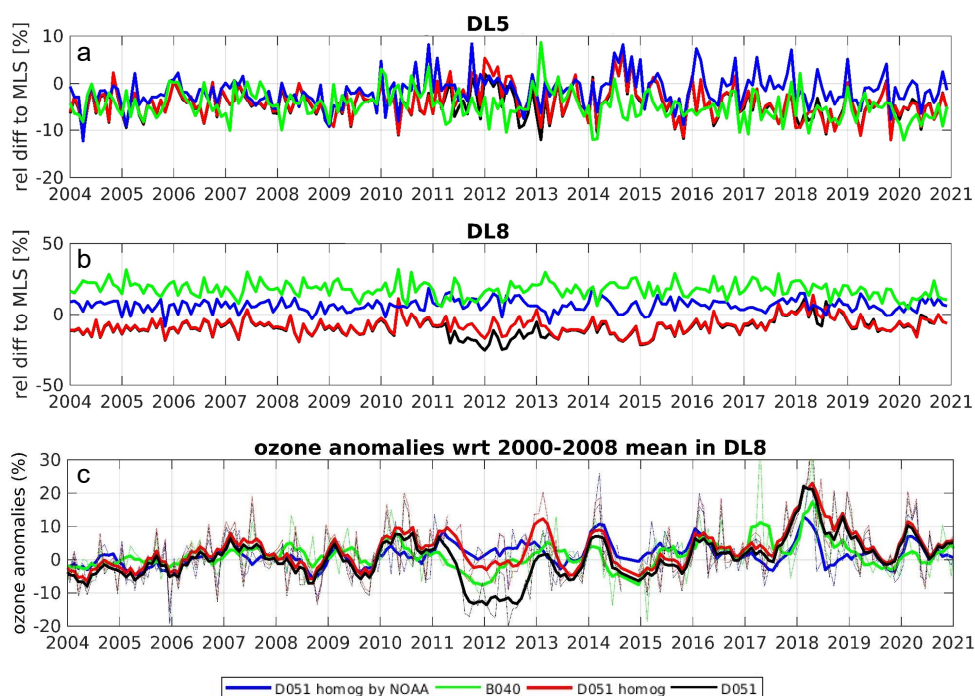


Figure 5. Monthly mean ozone content relative difference to Aura MLS for Dobson D051 as measured (black), Dobson D051 NOAA optimized (blue), Dobson D051 MCH homogenized (this study, red) and Brewer B040 (green) deseasonalized time series in (a) DL5 and (b) DL8. (c) Time series of ozone anomalies towards their 2000-2008 mean for the same ground-based datasets in DL8.

is reported in DL5. However, the slight underestimation of the MCH homogenization since 2017 seems to match the Brewer
290 B040 difference to Aura MLS in DL5. After 2017, the relative difference to Aura MLS of D051 homogenized by MCH and
of the collocated B040 is within -5% to -10% while the D051 homogenized by NOAA lies within -2% of Aura MLS. A clear
correction of the 2011-2013 period is visible in DL8. Except for the respective MCH and NOAA homogenized datasets mean
offsets to Aura MLS, a slight overestimation of the NOAA homogenization is visible in 2012 and 2013. However, the Brewer
B040 relative difference to Aura MLS is also slightly smaller during this time range, when the Brewer instrument had not
295 undergone any technical interventions. This is particularly visible on the anomalies time series of B040 in Fig. 5(c). As the
MCH homogenization relies on the Brewer collocated datasets, it allows to take into account the local variability of the ozone
DL8 content that the M2GMI model, base for the NOAA homogenization, probably does not consider.

In addition to the step correction in May 2018, the MCH homogenized dataset seems to show an anomaly in year 2018, as
the collocated Brewer B040 dataset. The NOAA homogenization considering a correction in 2017, the 2018 anomaly is taken
300 into account in the post-step period. The MCH homogenization considering a correction in May 2018, the 2018 anomaly is



taken into account in the pre- and post-step period. As a result, the calculated offsets differ, with a probable overestimation of the offset for the NOAA homogenization and a very small offset correction for the MCH homogenization.

4 Trend estimate methods

4.1 MLR trend estimate

305 Trends are estimated by fitting a multi-linear regression (MLR) function to the monthly mean ozone time series considering two piecewise linear ramps (PWL) starting in 1970 and in 2000. Trend profiles are obtained by considering one independent monthly mean time series for each pressure level. The results are given as a difference in DU to the 1970–1980 and of the 2000–2010 means. The explanatory variables represent sources of geophysical variability with known influence on stratospheric ozone, including the quasi-biennial oscillation¹ (QBO) at 30 and 10 hPa, the 10.7 cm solar radio flux describing the 11-
310 year solar cycle² (SOL), the El Niño–Southern Oscillation³ (ENSO), the North Atlantic Oscillation⁴ (NAO), the Stratospheric Aerosol Optical Depth⁵ (SAOD) and Fourier components representing the seasonal cycle (annual and semi-annual variations). All data points are considered with equal weights, and the uncertainty of the fit parameters is estimated from the regression residuals. Residual autocorrelations are accounted for by applying a Cochrane-Orcutt transformation to the model (Cochrane and Orcutt, 1949).

315 4.2 DLM trend estimate

Dynamic linear Modeling (DLM) allows the determination of a non-linear time-varying trend from a monthly means time series. This is a Bayesian approach regression which fits the data time series for a non-linear time-varying trend, regression coefficients from explanatory variables and seasonal and annual modes, considering their uncertainties and an autoregressive component. The trend is allowed to smoothly vary in time and its degree of non-linearity is inferred from the data, as well as the
320 turnaround period. We use the code by Alsing (2019) which is a Python implementation of the formalism introduced by Laine et al. (2014) and we refer to these publications for a detailed description of the DLM principles. The used model considers standard regression components, allows a variability of the sinusoidal seasonal modes and includes the autoregressive (AR1) correlation process with variance and correlation coefficient as free parameters in the regression. The same five explanatory variables as in the MLR are used in the trend estimate: QBO at 30hPa and 10hPa, SOL, ENSO and SAOD NH values. The
325 estimation of the posterior uncertainty distribution is performed with the Markov chain Monte Carlo (MCMC) method, and considers the uncertainties on the regression components, on the seasonal cycle, on the autoregressive correlation and on the non-linearity of the trend.

¹ from <http://www.spaceweather.gc.ca/solarflux/sx-5-mavg-eng.php>

² from <http://www.spaceweather.gc.ca/solarflux/sx-5-mavg-eng.php>

³ from <http://www.esrl.noaa.gov/psd/enso/mei/>

⁴ from <https://climatedataguide.ucar.edu/climate-data/hurrell-north-atlanticoscillation-nao-index-station-based>

⁵ from https://asdc.larc.nasa.gov/project/GloSSAC/GloSSAC_1.0

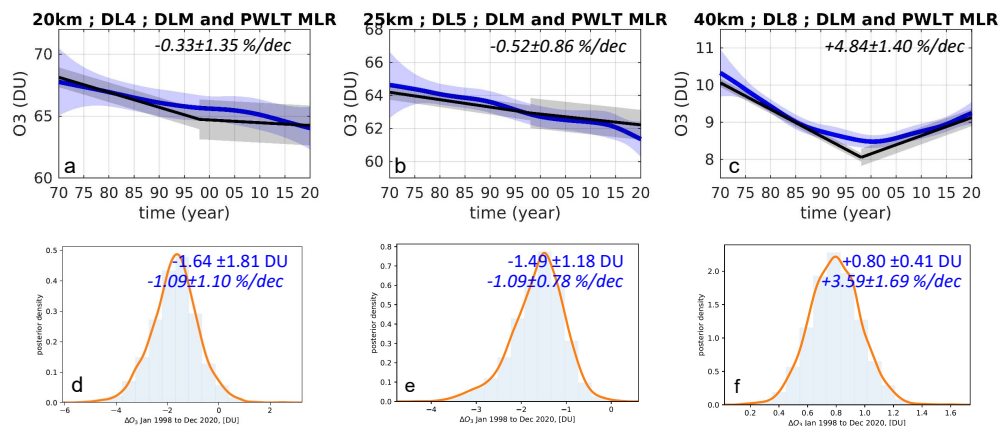


Figure 6. (a-c) DLM and MLR trend estimates in %/decade $\pm 2\sigma$ of Dobson D051 dataset for 3 DL between 20 and 40 km, the shaded areas show the 2σ uncertainties, (d-f) the distribution of the DLM trend estimates is given by the kernel density estimation (KDE) for the same 3 DL in the 1998–2020 time range in DU \pm FWHM.

Figure 6 shows the long-term trend estimates from the Dobson D051 dataset by DLM (in blue with ± 2 sigma uncertainty shaded area) and by MLR (PWT, in black with ± 2 sigma uncertainty shaded area) for the same explanatory variables at 3
 330 altitudes levels.

Overall trends are similar but differ over short timescales because of their representation of the nonlinearity of the changes in the data record. The advantage of DLM lies in the estimation of a smoothly varying trend without assuming any shape. The inflection year depends on the method: while the inflection point is fixed by the MLR PWT (1998 in this case, see Petropavlovskikh et al., 2019), the inflection year is retrieved by the DLM and results in year 2002 for the Dobson D051
 335 dataset above 28 km. The maximum of the ΔO_3 1998–2020 KDE (kernel density estimation) should be compared to the linear trend value over the same time period (22 years), while the 95% level of significance, represented by the fraction of the KDE above/below zero, slightly differs from the MLR uncertainty estimates. In the LS, for DL4 (Fig 6a and d), the post-2000 MLR trends values are -0.33 ± 1.35 %/decade. The DLM KDE shows a maximum at -1.64 DU and a FWHM (=2.4 sigma for normal distribution) of 1.81 DU, which means a mean trend of -1.09 ± 1.10 %/decade. MLR estimate is non significantly different from
 340 zero at the 95% confidence level while DLM estimate is negative barely significant at the 95% level. In the MS, for DL5 (Fig 6b and e), the post-2000 MLR trends values are -0.52 ± 0.86 %/decade. The DLM KDE shows a maximum at -1.49 DU and a FWHM of 1.18 DU, which means a mean trend of -1.09 ± 0.78 %/decade. MLR estimate is non significantly different from zero at the 95% confidence level while DLM estimate is significantly negative at the 95% level. In the UpS, for DL8 (Fig 6c and f), the post-2000 MLR trends values are $+4.84 \pm 1.40$ %/decade and the DLM KDE shows a maximum at $+0.80$ DU and a FWHM
 345 of 0.41 DU, which means a mean trend of $+3.59 \pm 1.69$ %/decade. Both are significantly positive at the 95% confidence level.

In case of high annual variability, a DLM trend estimate in %/decade may be significant while a MLR trend estimate may be non significant for the same considered period. The given DLM trend value in %/decade is an average of the % change

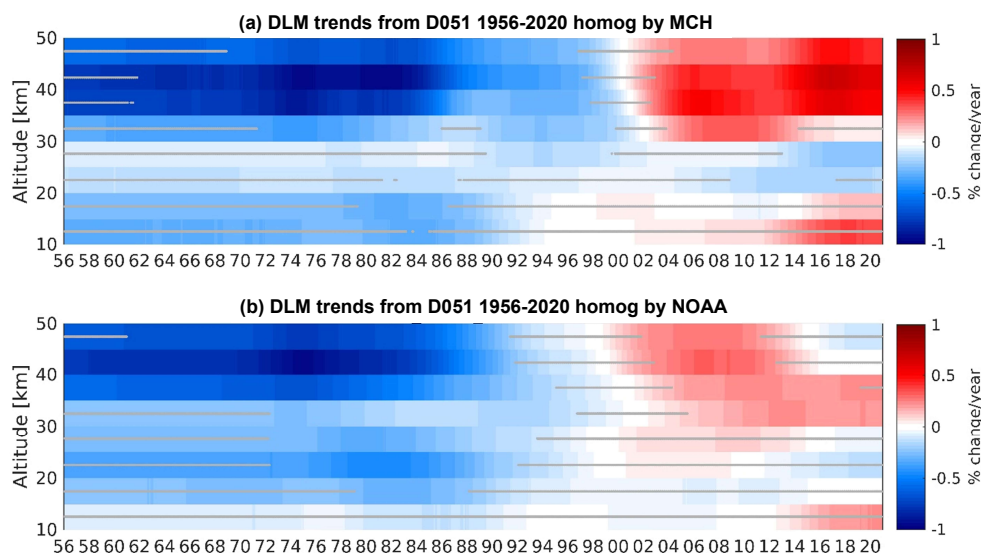


Figure 7. DLM trend estimates in %/year of Dobson D051 1956-2020 from (a) MCH homogenised and (b) NOAA optimized data records. Grey lines indicate trend estimates non significantly different from zero at the 95% confidence level.

per year. In a DLM estimate, only a limited number of values of % change per year may be influenced by an inhomogeneity, whereas the same inhomogeneity, especially when occurring at the boundaries of the time period considered, may influence the MLR trends significantly.

5 Results

Figure 7a and b shows the DLM trend estimates derived from the Dobson D051 record as homogenized by MCH (a, this study) and by NOAA (b). The trends values are given in % change per year for each altitude level between 10 and 50 km. Positive and negative trends are shown with varying intensities of red and blue respectively. The grey lines indicate trend estimates non significantly different from zero at the 95% confidence level.

The upper stratospheric (UpS, DL7-10, 10–1 hPa, 35–50 km) trend estimates are significantly negative between 1965 and 1997 on Figure 7a and before 1997 on Figure 7b. The mean negative trend estimates are -5 %/decade (mean value of the 1965-1997 UpS trends). Both records show then a transition period until 2003 with non-significant UpS trend estimates. The post-2003 UpS trends are significant and positive, up to 2020 for the MCH homogenized Dobson D051 record and until 2013 for the NOAA homogenized Dobson D051 record. The mean positive UpS trends are 3.6 %/decade on Figure 7a (mean value of the 2003-2013 UpS trends) and 2.1 %/decade on Figure 7b (mean value of the 2003-2013 UpS trends). Note that due to the large AVK of the Umkehr measurement, the ozone and trend informations in DL8 and DL9 are not independent. In the middle stratosphere (MS, DL5&6, 24–32 km), both homogenized records show a negative trend, persistent and significantly

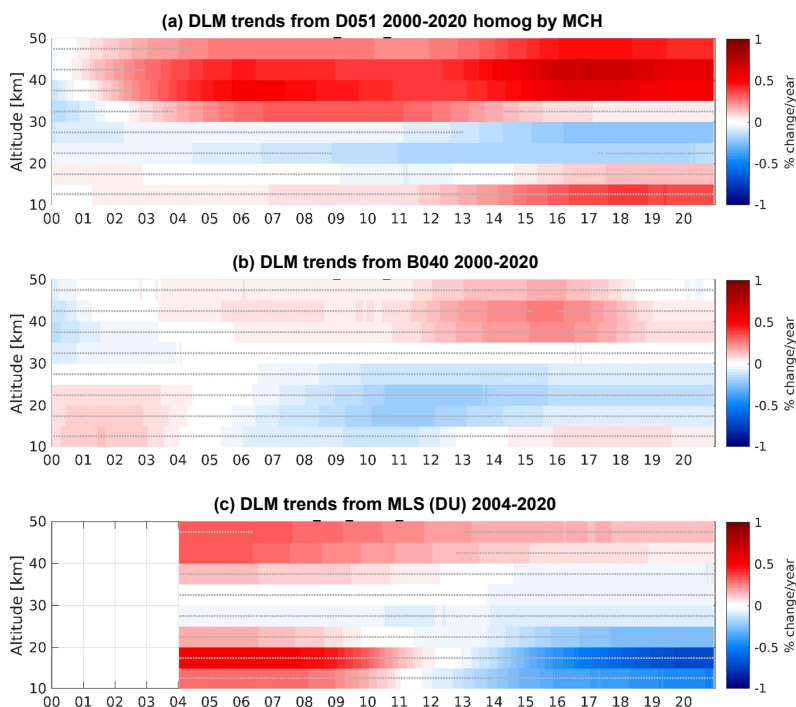


Figure 8. post 2000 DLM trend estimates in %/year from (a) Dobson D051, (b) Brewer B040 and (c) Aura MLS data records.

different from zero at the 95% confidence level since 2012 for the MCH homogenized Dobson D051 data record but slightly
365 positive between 2002 and 2010 and non significantly different from zero at the 95% confidence level for the NOAA optimized
data record. The lower stratospheric (LS, DL3&4, 14-24 km) trend estimates are non significantly negative before 1996 but
significantly negative between 2008 and 2018 for the MCH homogenized data record and non significantly negative for the
NOAA homogenized Dobson D051 record.

Again due to the AVKs width of the Umkehr profiles, the ozone content information of DL2 partly overpasses the LS as
370 usually defined (see representation of shaded areas in Figure 1b). The same consideration is true for the DL6 and the MS. The
lower part of the LS and the upper part of the MS trends may be aliased by upper tropospheric respectively upper stratospheric
information.

Post-2000 trend have been estimated on the 3 Dobson and the 3 Brewer MCH Umkehr data records. The trends estimates of
one of the Dobsons (D051) and one of the Brewers (B040) are represented in Figure 8 a and b in % change per year for each
375 altitude level between 10 and 50 km.

The post-2000 trends show similar features for the two Swiss spectrophotometers:

- a positive trend of 0.2 to 0.5 %/year above 35 km, significant for Dobson D051 (and for Dobson D062 and Brewer B156 not shown) but lower and therefore non significantly different from zero at the 95% level of confidence for Brewer B040 and



Dobson D101. Despite differences in the trend estimates intensities, an overall picture of a UpS positive trend after 2002 is
380 shown.

- a persistent negative trend in the middle and the lower stratosphere with different levels of significance depending on the dataset but mostly non significantly different from zero at the 95% confidence level except for Dobson D051.

Significant UpS positive trends are estimated on the Aura MLS satellite data record (Figure 8c) however non significant since 2013. Signs of negative trends in the lower altitudes are also observed although not significant: DLM trend estimates are
385 persistently negative in the MS and negative in the LS since 2012.

Both the Boulder D067 and the OHP D085 have been homogenized by NOAA towards M2GMI (Petropavlovskikh et al., 2022) and both data records are used for MLR trend derivation in LOTUS (Godin-Beekmann et al., 2022). D067, D085 (not shown) and Dobson D051 homogenized by NOAA show similar upper stratospheric post-2000 trends i.e. a statistically significant positive trend followed by a non significant negative trend, with a transition in 2014 for D067, in 2016 for Dobson
390 D051 and in 2017 for D085. The LS trends are non significant and are not persistently negative.

6 Conclusions

Data records of six collocated spectrophotometers were inter-compared on the observation data level and on the ozone profile level in order to detect anomalies. The MCH Dobson D051 Umkehr data record has been homogenized on the observation data level by comparison to the collocated Brewer triad data record and to the redundant Dobson data records. In parallel, a second
395 homogenization of the same Dobson dataset was performed by NOAA, using comparison with the M2GMI model on the raw data level as well. Both homogenizations result in similar magnitudes of N values corrections relative to the post 2018 values if we exclude the volcanic eruption periods for which corrections are performed by the NOAA optimization process but during which data are not considered in the MCH homogenization. On the other hand, by relying on the collocated Brewers datasets, the MCH homogenization accounts for the local variability of the ozone layers content in the 2011-2013 period and results in
400 a weaker correction of the data record for this period.

Even if only slightly different, the homogenizations of the raw data can produce significant differences in ozone profiles and, therefore, in the long term trend estimates. When compared to Aura MLS and to Brewer B040, both homogenizations differ in the ozone profiles level in the UpS, especially for the period 2017-2019.

Trends of the ozone profile time series have been estimated by DLM from the Dobson and the Brewer spectrophotometers
405 datasets. The post-2000 trends show similar features namely a positive trend of 0.2 to 0.5 %/year above 35 km in the UpS, significant for Dobson D051 but lower and therefore non significantly different from zero at the 95% level of confidence for Brewer B040, and a persistent negative trend in the MS with different levels of significance depending on the dataset. The DLM trend estimates from Dobson D051 show a significant persistent negative trend in the MS and supports also the mention of a persistent negative trend in NH LS when measured by ground-based instrument, considering, however, that the trends
410 estimates in the upper part of the MS and in the lower part of the LS are aliased by the large AVKs of the Umkehr profiles.



DLM trend estimates derived from Aura MLS show similar features in the UpS and the MS as estimates from the ground-based Dobson and Brewer spectrophotometers. However, a transition from non significant positive to non significant negative trends in the LS remains unexplained.

415 While significant positive trends have been estimated in the UpS since 2004 from the MCH homogenized Dobson D051 dataset, the trend estimates from the NOAA optimized data record appear to show a transition from significant positive to non-significant negative/zero values above 40 km in 2016. Further investigation will be needed to confirm this transition and exclude 2017 as a problematic period in the NOAA homogenization.

420 Both homogenization approaches considered in this study are relevant and significantly improve the Dobson D051 data record. However, inconsistencies in the level of significance of the Dobson D051 trend estimates are noticed and should be attributed to the remaining differences left by the homogenizations in the data records.

425 *Data availability.* The as measured Dobson D051 dataset is available at WOUDC. The NOAA homog Dobson D051 dataset is available at <https://gml.noaa.gov/aftp/data/ozwv/Dobson/AC4/Umkehr/Optimized/Daily/ARO/>. The MCH homogenized Dobson D051 dataset, the Dobson D062, Dobson D101 and the Brewers Umkehr datasets can be obtained from EMB on request. The MLS ozone dataset is available from the NASA Goddard Space Flight Center Earth Sciences Data and Information Services Center (GES DISC) at <http://disc.sci.gsfc.nasa.gov/Aura/data-holdings/MLS/index.shtml>.

430 *Author contributions.* E.M.B. is responsible for the Umkehr ozone measurements with the Arosa/Davos Dobson and Brewer spectrophotometers, performed the data analysis and prepared the manuscript. A.H. and R.S. contributed to the interpretation of the results. A.J. performed the 2011-2013 homogenisation and the first DLM trend derivation. H.S. is responsible for the Arosa/Davos Dobson and Brewer spectrophotometers. I.P. and K.M. performed the NOAA homogenization of D051. M.S. implemented the Umkehr Brewer retrieval algorithm. L.F. is responsible for the Aura MLS measurements. All co-authors contributed to the preparation of the manuscript.

Competing interests. The authors have no competing interests.

435 *Acknowledgements.* This work has been funded by MeteoSwiss within the Swiss Global Atmospheric Watch program of the World Meteorological Organization (GAW-CH 2018-2021). Work performed at the Jet Propulsion Laboratory, California Institute of Technology, was performed under contract with the National Aeronautics and Space Administration. Work performed at NOAA has been supported by the Climate Program Office (grant no. NA19OAR4310169).



References

- The Montreal Protocol on Substances that Deplete the Ozone Layer, International Legal Materials, 26, <https://ozone.unep.org/treaties/montreal-protocol/montreal-protocol-substances-deplete-ozone-layer>, 1987.
- Alsing, J.: dlmmc: Dynamical linear model regression for atmospheric time-series analysis, *Journal of Open Source Software*, 4, 1157, <https://doi.org/10.21105/joss.01157>, 2019.
- 440 Arosio, C., Rozanov, A., Malinina, E., Weber, M., and Burrows, P. J.: Merging of ozone profiles from SCIAMACHY, OMPS and SAGE II observations to study stratospheric ozone changes, *Atmospheric Measurement Techniques*, 12, 2423–2444, <https://doi.org/10.5194/amt-12-2423-2019>, 2019.
- Ball, W. T., Alsing, J., Mortlock, D. J., Rozanov, E. V., Tummon, F., and Haigh, J. D.: Reconciling differences in stratospheric ozone
445 composites, *Atmospheric Chemistry and Physics*, 17, 12 269–12 302, <https://doi.org/10.5194/acp-17-12269-2017>, 2017.
- Ball, W. T., Alsing, J., Mortlock, D. J., Staehelin, J., Haigh, J. D., Peter, T., Tummon, F., Stübi, R., Stenke, A., Anderson, J., Bourassa, A., Davis, S. M., Degenstein, D., Frith, S., Froidevaux, L., Roth, C., Sofieva, V., Wang, R., Wild, J., Yu, P., Ziemke, J. R., and Rozanov, E. V.: Evidence for a continuous decline in lower stratospheric ozone offsetting ozone layer recovery, *Atmospheric Chemistry and Physics*, 18, 1379–1394, <https://doi.org/10.5194/acp-18-1379-2018>, 2018.
- 450 Ball, W. T., Alsing, J., Staehelin, J., Davis, S. M., Froidevaux, L., and Peter, T.: Stratospheric ozone trends for 1985–2018: sensitivity to recent large variability, *Atmospheric Chemistry and Physics*, 10, 12 731–12 748, <https://doi.org/10.5194/acp-19-12731-2019>, 2019.
- Basher, R.: Review of the Dobson spectrophotometer and its accuracy, Global Ozone Research and Monitoring Project–Report No. 13, 81pp., <https://gml.noaa.gov/ozwv/dobson/papers/report13/report13.html>, 1982.
- Bernet, L., von Clarmann, T., Godin-Beekmann, S., Ancellet, G., Maillard Barras, E., Stübi, R., Steinbrecht, W., Kämpfer, N., and Hocke, K.:
455 Ground-based ozone profiles over central Europe: incorporating anomalous observations into the analysis of stratospheric ozone trends, *Atmospheric Chemistry and Physics*, 19, 4289–4309, <https://doi.org/10.5194/acp-19-4289-2019>, 2019.
- Bhartia, P. K., McPeters, R. D., Flynn, L. E., Taylor, S., Kramarova, N. A., Frith, S., Fisher, B., and Deland, M.: Solar backscatter UV (SBUV) total ozone and profile algorithm, *Atmospheric Measurement Techniques*, 6, 2533–2548, <https://doi.org/10.5194/amt-6-2533-2013>, 2013.
- Bognar, K., Tegtmeier, S., Bourassa, A., Roth, C., Warnok, T., Zawada, D., and Degenstein, D.: Stratospheric ozone trends for 1984–2021 in
460 the SAGE II – OSIRIS– SAGE III/ISS composite dataset, *Atmos. Chem. Phys. Discuss.*, <https://doi.org/https://doi.org/10.5194/acp-2022-252>, 2022.
- Chipperfield, M. P., Dhomse, S., Hossaini, R., Feng, W., Santee, M. L., Weber, M., Burrows, J. P., Wild, J. D., Loyola, D., and Coldewey-Egbers, M.: On the Cause of Recent Variations in Lower Stratospheric Ozone, *Geophysical Research Letters*, 45, 5718–5726, <https://doi.org/10.1029/2018GL078071>, 2018.
- 465 Cochran, D. and Orcutt, G. H.: Application of least squares regression to relationships containing auto-correlated error terms, *J. Am. Stat. Assoc.*, 44, 32–61, 1949.
- Dietmüller, S., Garny, H., Eichinger, R., and Ball, W. T.: Analysis of recent lower-stratospheric ozone trends in chemistry climate models, *Atmospheric Chemistry and Physics*, 21, 6811–6837, <https://doi.org/10.5194/acp-21-6811-2021>, 2021.
- Evans, R., Petropavlovskikh, I., McClure-Begley, A., McConville, G., Quincy, D., and Miyagawa, K.: Technical note: The US Dobson
470 station network data record prior to 2015, re-evaluation of NDACC and WOUDC archived records with WinDobson processing software, *Atmospheric Chemistry and Physics*, 17, 12 051–12 070, 2017.



- Fragkos, K. I. P., Dotsas, M., Bais, A., Taylor, M., Hurtmans, D., Fountoulakis, I., Koukouli, M. E., Balis, D., and Stanek, M.: Umkehr ozone profiles over Thessaloniki and comparison with satellite overpasses, in: 20th EGU General Assembly 2018, Vienna, Austria, 2018.
- Garane, K., Koukouli, M., Fragkos, K., Miyagawa, K., Fountoukidis, P., Petropavlovskikh, I., Balis, D., and Bais, A.: Umkehr Ozone Profile Analysis and Satellite Validation, ESA project WP-2190, <https://zenodo.org/record/5584472>, 2022.
- 475 Gelaro, R., McCarty, W., Suárez, M. J., Todling, R., Molod, A., Takacs, L., Randles, C. A., Darmenov, A., Bosilovich, M. G., Reichle, R., Wargan, K., Coy, L., Cullather, R., Draper, C., Akella, S., Buchard, V., Conaty, A., da Silva, A. M., Gu, W., Kim, G. K., Koster, R., Lucchesi, R., Merkova, D., Nielsen, J. E., Partyka, G., Pawson, S., Putman, W., Rienecker, M., Schubert, S. D., Sienkiewicz, M., and Zhao, B.: The modern-era retrospective analysis for research and applications, version 2 (MERRA-2), *Journal of Climate*, 30, 5419–5454, <https://doi.org/10.1175/JCLI-D-16-0758.1>, 2017.
- 480 Godin-Beekmann, S., Azouz, N., Sofieva, V., Hubert, D., Petropavlovskikh, I., Effertz, P., Ancellet, G., Degenstein, D., Zawada, D., Froidevaux, L., Frith, S., Wild, J., Davis, S., Steinbrecht, W., Leblanc, T., Querel, R., Tourpali, K., Damadeo, R., Maillard Barras, E., Stübi, R., Vigouroux, C., Arosio, C., Nedoluha, G., Boyd, I., and van Malderen, R.: Updated trends of the stratospheric ozone vertical distribution in the 60° S–60° N latitude range based on the LOTUS regression model, *Atmos. Chem. Phys.*, <https://doi.org/10.5194/acp-2022-137>, 2022.
- 485 Gröbner, J., Schill, H., Egli, L., and Stübi, R.: Consistency of total column ozone measurements between the Brewer and Dobson spectroradiometers of the LKO Arosa and PMOD/WRC Davos, *Atmospheric Measurement Techniques*, 14, 3319–3331, <https://doi.org/10.5194/amt-14-3319-2021>, 2021.
- Harris, N. R., Hassler, B., Tummon, F., Bodeker, G. E., Hubert, D., Petropavlovskikh, I., Steinbrecht, W., Anderson, J., Bhartia, P. K., Boone, C. D., Bourassa, A., Davis, S. M., Degenstein, D., Delcloo, A., Frith, S. M., Froidevaux, L., Godin-Beekmann, S., Jones, N., Kurylo, M. J., Kyrölä, E., Laine, M., Leblanc, S. T., Lambert, J. C., Liley, B., Mahieu, E., Maycock, A., De Mazière, M., Parrish, A., Querel, R., Rosenlof, K. H., Roth, C., Sioris, C., Staehelin, J., Stolarski, R. S., Stübi, R., Tamminen, J., Vigouroux, C., Walker, K. A., Wang, H. J., Wild, J., and Zawodny, J. M.: Past changes in the vertical distribution of ozone - Part 3: Analysis and interpretation of trends, *Atmospheric Chemistry and Physics*, 15, 9965–9982, <https://doi.org/10.5194/acp-15-9965-2015>, 2015.
- 490 Kyrölä, E., Laine, M., Sofieva, V., Tamminen, J., Pivrinta, S. M., Tukiainen, S., Zawodny, J., and Thomason, L.: Combined SAGE II-GOMOS ozone profile data set for 1984-2011 and trend analysis of the vertical distribution of ozone, *Atmospheric Chemistry and Physics*, 13, 10645–10658, <https://doi.org/10.5194/acp-13-10645-2013>, 2013.
- Laine, M., Latva-Pukkila, N., and Kyrölä, E.: Analysing time-varying trends in stratospheric ozone time series using the state space approach, *Atmospheric Chemistry and Physics*, 14, 9707–9725, <https://doi.org/10.5194/acp-14-9707-2014>, 2014.
- 500 Livesey, N. J., Read, W. G., Wagner, P. A., Froidevaux, L., Lambert, A., Manney, G. L., Millán Valle, L. F., Pumphrey, H. C., Santee, M. L., Schwartz, M. J., Wang, S., Fuller, R. A., Jarnot, R. F., Knosp, B. W., Martinez, E., and Lay, R. R.: Earth Observing System (EOS) Aura Microwave Limb Sounder (MLS) Version 4.2x Level 2 data quality and description document, pp. 1–168, https://mls.jpl.nasa.gov/data/v4-2_data_quality_document.pdf, 2018.
- Maillard, E., Schill, H., Stübi, R., and Ruffieux, D.: Re-evaluation of Arosa Umkehr serie: ozone profile measurements from 1931 up to now, in: paper presented at Quadrennial Ozone Symposium, Tromsø, Norway, June 29th - July 5th, 2008.
- 505 Maillard Barras, E., Haeferle, A., Nguyen, L., Tummon, F., Ball, W., Rozanov, E., Rüfenacht, R., Hocke, K., Bernet, L., Kämpfer, N., Nedoluha, G., and Boyd, I.: Study of the dependence of stratospheric ozone long-term trends on local solar time, *Atmospheric Chemistry and Physics*, 20, 8453–8471, <https://doi.org/10.5194/acp-2020-101>, 2020.
- Mateer, C. L.: On the information content of Umkehr observations, *J. Atmos. Sci.*, 22, 370–382, 1965.



- 510 McPeters, R., Hollandsworth, S.M. and Flynn, L., Herman, J., and Seftor, C.: Long-term ozone trends derived from the 16 year combined Nimbus 7/Meteor 3 TOMS Version 7 Record, *Geophysical Research Letters*, 23, 3699–3702, <https://doi.org/10.1029/96GL03540>, 1996a.
- McPeters, R. D. and Labow, G. J.: Climatology 2011: An MLS and sonde derived ozone climatology for satellite retrieval algorithms, *Journal of Geophysical Research Atmospheres*, 117, <https://doi.org/10.1029/2011JD017006>, 2012.
- McPeters, R. D., Bhartia, P. K., Krueger, A. J., Herman, J. R., Schlesinger, B. M., Wellemeyer, C. G., Seftor, C. J., Jaross, G., Taylor, S. L.,
515 Swisler, T., Torres, O., Labow, G., Byerly, W., and Cebula, R. P.: Nimbus-7 Total Ozone Mapping Spectrometer Data Products User's Guide, NASA Ref. Publ., p. 75, 1996b.
- Miller, A. J., Tiao, G., Reinsel, G., Wuebbles, D., Bishop, L., Kerr, J., Nagatani, R., DeLuisi, J., and Mateer, C.: Comparisons of observed ozone trends in the stratosphere through examination of Umkehr and balloon ozonesonde data, *Journal of Geophysical Research*, 100, 11 209–11 217, <https://doi.org/10.1029/95jd00632>, 1995.
- 520 Orbe, C., Oman, L. D., Strahan, S. E., Waugh, D. W., Pawson, S., Takacs, L. L., and Molod, A. M.: Large-Scale Atmospheric Transport in GEOS Replay Simulations, *Journal of Advances in Modeling Earth Systems*, 9, 2545–2560, <https://doi.org/10.1002/2017MS001053>, 2017.
- Orbe, C., Wargan, K., Pawson, S., and Oman, L. D.: Mechanisms Linked to Recent Ozone Decreases in the Northern Hemisphere Lower Stratosphere, *Journal of Geophysical Research: Atmospheres*, 125, 1–23, <https://doi.org/10.1029/2019JD031631>, 2020.
- 525 Park, A., Guillas, S., and Petropavlovskikh, I.: Trends in stratospheric ozone profiles using functional mixed models, *Atmospheric Chemistry and Physics*, 13, 11 473–11 501, <https://doi.org/10.5194/acp-13-11473-2013>, 2013.
- Petropavlovskikh, I., Bhartia, P. K., and DeLuisi, J.: New Umkehr ozone profile retrieval algorithm optimized for climatological studies, *Geophysical Research Letters*, 32, 1–5, <https://doi.org/10.1029/2005GL023323>, 2005a.
- Petropavlovskikh, I., Kireev, S., Maillard, E., Stuebi, R., and Bhartia, P. K.: New Brewer algorithm for a single pair, WMO TD No. 1419,
530 25–27, https://library.wmo.int/doc_num.php?explnum_id=9374, 2005b.
- Petropavlovskikh, I., Evans, R., McConville, G., Oltmans, S., Quincy, D., Lantz, K., Disterhoft, P., Stanek, M., and Flynn, L.: Sensitivity of Dobson and Brewer Umkehr ozone profile retrievals to ozone cross-sections and stray light effects, *Atmospheric Measurement Techniques*, 4, 1841–1853, <https://doi.org/10.5194/amt-4-1841-2011>, 2011.
- Petropavlovskikh, I., Godin-Beekmann, S., Hubert, D., Damadeo, R. P., Hassler, B., Sofieva, V. F., Frith, S. M., and Tourpali, K.:
535 SPARC/IOC/GAW report on Long-term Ozone Trends and Uncertainties in the Stratosphere, Report No. 9, GAW Report No. 241, WCRP-17/2018, <https://doi.org/10.17874/f899e57a20b>, 2019.
- Petropavlovskikh, I., Miyagawa, K., McClure-Beegle, A., Johnson, B., Wild, J., Strahan, S., Wargan, K., Querel, R., Flynn, L., Beach, E., G., A., and Godin-Beekmann, S.: Optimized Umkehr profile algorithm for ozone trend analyses, *Atmospheric Measurement Techniques*, 15, <https://doi.org/https://doi.org/10.5194/amt-15-1849-2022>, 2022.
- 540 Randel, W., Stolarski, R., Cunnold, D., Logan, J., Newchurch, M., and Zawodny, J.: Trends in the vertical distribution of ozone, *Science*, 285, 1689–1692, 1999.
- Reinsel, G. C., Tiao, G. C., DeLuisi, J. J., Basu, S., and Carriere, K.: Trend analysis of aerosol-corrected Umkehr ozone profile data through 1987, *Journal of Geophysical Research*, 94, <https://doi.org/10.1029/jd094id13p16373>, 1989.
- Reinsel, G. C., Weatherhead, E., Tiao, G. C., Miller, A. J., Nagatani, R. M., Wuebbles, D. J., and Flynn, L. E.: On detection of turnaround
545 and recovery in trend for ozone, *Journal of Geophysical Research: Atmospheres*, 107, <https://doi.org/10.1029/2001JD000500>, 2002.
- Rodgers, C. D.: Inverse Methods for Atmospheric Sounding - Theory and Practice, vol. 2 of *Series on Atmospheric Oceanic and Planetary Physics*, World Scientific Publishing Co. Pte. Ltd., Singapore, <https://doi.org/10.1142/9789812813718>, 2000.



- Serdyuchenko, A., Gorshelev, V., Weber, M., Chehade, W., and Burrows, J. P.: High spectral resolution ozone absorption cross-sections – Part 2: Temperature dependence, *Atmospheric Measurement Techniques*, 7, 625–636, <https://doi.org/10.5194/amt-7-625-2014>, 2014.
- 550 Smit, H. G., Straeter, W., Johnson, B. J., Oltmans, S. J., Davies, J., Tarasick, D. W., Hoegger, B., Stubi, R., Schmidlin, F. J., Northam, T., Thompson, A. M., Witte, J. C., Boyd, I., and Posny, F.: Assessment of the performance of ECC-ozonesondes under quasi-flight conditions in the environmental simulation chamber: Insights from the Juelich Ozone Sonde Intercomparison Experiment (JOSIE), *Journal of Geophysical Research Atmospheres*, 112, <https://doi.org/10.1029/2006JD007308>, 2007.
- Sofieva, V. F., Szelag, M., Tamminen, J., Kyrölä, E., Degenstein, D., Roth, C., Zawada, D., Rozanov, A., Arosio, C., Burrows, J. P., Weber, 555 M., Laeng, A., Stiller, G. P., Von Clarmann, T., Froidevaux, L., Livesey, N., Van Roozendaal, M., and Retscher, C.: Measurement report: Regional trends of stratospheric ozone evaluated using the Merged GRIdded Dataset of Ozone Profiles (MEGRIDOP), *Atmospheric Chemistry and Physics*, 21, 6707–6720, <https://doi.org/10.5194/acp-21-6707-2021>, 2021.
- Stahelin, J., Harris, N. R. P., Appenzeller, C., and Eberhard, J.: Ozone trends: a review, *Reviews of Geophysics*, 39, 231–290, 2001.
- Stahelin, J., Kerr, J., Evans, R., and Vanicek, K.: Comparison of total ozone measurements of Dobson and Brewer spectrophotometers and 560 recommended transfer functions, https://library.wmo.int/doc/_num.php?explnum_{_}id=9226, 2003.
- Stahelin, J., Viatte, P., Stübi, R., Tummon, F., and Peter, T.: Stratospheric ozone measurements at Arosa (Switzerland): History and scientific relevance, *Atmospheric Chemistry and Physics*, 18, 6567–6584, <https://doi.org/10.5194/acp-18-6567-2018>, 2018.
- Steinbrecht, W., Froidevaux, L., Fuller, R., Wang, R., Anderson, J., Roth, C., Bourassa, A., Degenstein, D., Damadeo, R., Zawodny, J., Frith, S., McPeters, R., Bhartia, P., Wild, J., Long, C., Davis, S., Rosenlof, K., Sofieva, V., Walker, K., Rahpoe, N., Rozanov, A., Weber, 565 M., Laeng, A., von Clarmann, T., Stiller, G., Kramarova, N., Godin-Beekmann, S., Leblanc, T., Querel, R., Swart, D., Boyd, I., Hocke, K., Kämpfer, N., Maillard Barras, E., Moreira, L., Nedoluha, G., Vigouroux, C., Blumenstock, T., Schneider, M., García, O., Jones, N., Mahieu, E., Smale, D., Kotkamp, M., Robinson, J., Petropavlovskikh, I., Harris, N., Hassler, B., Hubert, D., and Tummon, F.: An update on ozone profile trends for the period 2000 to 2016, *Atmospheric Chemistry and Physics*, 17, 10 675–10 690, <https://doi.org/10.5194/acp-17-10675-2017>, 2017.
- 570 Stübi, R., Schill, H., Klausen, J., Vuilleumier, L., Gröbner, J., Egli, L., and Ruffieux, D.: On the compatibility of Brewer total column ozone measurements in two adjacent valleys (Arosa and Davos) in the Swiss Alps, *Atmospheric Measurement Techniques*, 10, 4479–4490, <https://doi.org/10.5194/amt-10-4479-2017>, 2017a.
- Stübi, R., Schill, H., Klausen, J., Vuilleumier, L., and Ruffieux, D.: Reproducibility of total ozone column monitoring by the Arosa Brewer spectrophotometer triad, *Journal of Geophysical Research: Atmospheres*, 122, 4735–4745, <https://doi.org/10.1002/2016JD025735>, 2017b.
- 575 Stübi, R., Schill, H., Klausen, J., Maillard Barras, E., and Haeefe, A.: A fully automated Dobson sun spectrophotometer for total column ozone and Umkehr measurements, *Atmospheric Measurement Techniques*, 14, 5757–5769, <https://doi.org/10.5194/amt-14-5757-2021>, 2021a.
- Stübi, R., Schill, H., Maillard Barras, E., Klausen, J., and Haeefe, A.: Quality assessment of Dobson spectrophotometers for ozone column measurements before and after automation at Arosa and Davos, *Atmospheric Measurement Techniques*, 14, 4203–4217, 580 <https://doi.org/10.5194/amt-14-4203-2021>, 2021b.
- Tarasick, D., Galbally, I. E., Cooper, O. R., Schultz, M. G., Ancellet, G., Leblanc, T., Wallington, T. J., Ziemke, J., Liu, X., Steinbacher, M., Stahelin, J., Vigouroux, C., Hannigan, J. W., García, O., Foret, G., Zanis, P., Weatherhead, E., Petropavlovskikh, I., Worden, H., Osman, M., Liu, J., Chang, K. L., Gaudel, A., Lin, M., Granados-Muñoz, M., Thompson, A. M., Oltmans, S. J., Cuesta, J., Dufour, G., Thouret, V., Hassler, B., Trickl, T., and Neu, J. L.: Tropospheric ozone assessment report: Tropospheric ozone from 1877 to 2016, observed levels, 585 trends and uncertainties, *Elementa*, 7, 1–56, <https://doi.org/10.1525/elementa.376>, 2019.



- Tummon, F., Hassler, B., Harris, N. R., Staehelin, J., Steinbrecht, W., Anderson, J., Bodeker, G. E., Bourassa, A., Davis, S. M., Degenstein, D., Frith, S. M., Froidevaux, L., Kyrölä, E., Laine, M., Long, C., Penckwitt, A. A., Sioris, C. E., Rosenlof, K. H., Roth, C., Wang, H. J., and Wild, J.: Intercomparison of vertically resolved merged satellite ozone data sets: Interannual variability and long-term trends, *Atmospheric Chemistry and Physics*, 15, 3021–3043, <https://doi.org/10.5194/acp-15-3021-2015>, 2015.
- 590 Wargan, K., Orbe, C., Pawson, S., Ziemke, J. R., Oman, L. D., Olsen, M. A., Coy, L., and Emma Knowland, K.: Recent Decline in Extratropical Lower Stratospheric Ozone Attributed to Circulation Changes, *Geophysical Research Letters*, 45, 5166–5176, <https://doi.org/10.1029/2018GL077406>, 2018.
- Waters, J., Froidevaux, L., Harwood, R., Jarnot, R., Pickett, H., Read, W., Siegel, P., Cofield, R., Filipiak, M., Flower, D., Holden, J., Lau, G., Livesey, N., Manney, G., Pumphrey, H., Santee, M., Wu, D., Cuddy, D., Lay, R., Loo, M., Perun, V., Schwartz, M., Stek, P., Thurstans, R.,
595 Boyles, M., Chandra, K., Chavez, M., Gun-Shing Chen, Chudasama, B., Dodge, R., Fuller, R., Girard, M., Jiang, J., Yibo Jiang, Knosp, B., LaBelle, R., Lam, J., Lee, K., Miller, D., Oswald, J., Patel, N., Pukala, D., Quintero, O., Scaff, D., Van Snyder, W., Tope, M., Wagner, P., and Walch, M.: The Earth observing system microwave limb sounder (EOS MLS) on the aura Satellite, *IEEE Transactions on Geoscience and Remote Sensing*, 44, 1075–1092, <https://doi.org/10.1109/TGRS.2006.873771>, 2006.
- WMO: SPARC/IOC/GAW Assessment of trends in the vertical distribution of ozone, *Stratospheric Processes and Their Role in Climate*,
600 Global Ozone Research and Monitoring Project–Report No. 43, eds Harris, N., Hudson, R. and Phillips, C., 289pp., Geneva, Switzerland, 1998.
- Zanis, P., Maillard, E., Staehelin, J., Zerefos, C., Kosmidis, E., Tourpali, K., and Wohltmann, I.: On the turnaround of stratospheric ozone trends deduced from the reevaluated Umkehr record of Arosa, Switzerland, *Journal of Geophysical Research Atmospheres*, 111, 1–15, <https://doi.org/10.1029/2005JD006886>, 2006.
- 605 Ziemke, J., Strode, S., Douglass, A., Joiner, J., Vasilkov, A., Oman, L., Liu, J., Strahan, S., Bhartia, P., and Haffner, D.: A cloud-ozone data product from Aura OMI and MLS satellite measurements, pp. 4067–4078, <https://doi.org/10.5194/amt-10-4067-2017>, 2017.